Environmental factors controlling the phytoplankton blooms at the Patagonia shelf-break in spring

Virginia M.T. Garcia [a,*], Carlos A.E. Garcia [b], Mauricio M. Mata [b], Ricardo C. Pollery [c], Alberto R. Piola [d,e], Sergio R. Signorini [f], Charles R. McClain [f], M. Débora Iglesias-Rodriguez [g]

[a] Department of Oceanography, Federal University of Rio Grande, Av. Italia, Km 8, Rio Grande, RS 96201-900, Brazil
[b] Department of Physics, Federal University of Rio Grande, Av. Italia, Km 8, Rio Grande, RS 96201-900, Brazil
[c] Institute of Biological and Environmental Sciences, Universidade Santa Úrsula, Rua Jornalista Orlando Dantas, 59, Rio de Janeiro, RJ 22231-010, Brazil
[d] Servicio de Hidrografia Naval, Av. Montes de Oca, 2124, Buenos Aires 1271, Argentina
[e] Universidad de Buenos Aires, Argentina
[f] NASA Goddard Space Flight Center, Code 614.8, Greenbelt Road, Greenbelt, MD 20771, USA
[g] School of Ocean and Earth Science, National Oceanography Centre, University of Southampton, European Way, Southampton SO14 3ZH, UK

ARTICLE INFO

ABSTRACT

The shelf-break front formed between Argentinean shelf waters and the Malvinas Current (MC) flow shows a conspicuous band of high phytoplankton biomass throughout spring and summer, detected by ocean color sensors. That area is the feeding and spawning ground of several commercial species of fish and squid and is thought to play an important role in CO_2 sequestration by the ocean. Phytoplankton blooms in this area have been attributed mainly to coccolithophorids, a group of calcite-producing phytoplankton. Here we present the environmental factors associated with the spring bloom at the Patagonian shelf-break ($40°$–$48°$S) in the austral spring 2004. A remarkable bloom of diatoms and dinoflagellates (approximately 1200 km long) was observed along the front, where integrated chlorophyll values ranged from 90.3 to 1074 mg m^{-2}. It is suggested that supply of macro-nutrients by upwelling and probably iron by both upwelling and shelf transport contribute to maintaining the spring bloom. Strong water column stability along the front allowed the accumulation of algal cells mainly in the top 50 m and their maintenance in the euphotic layer. East of the shelf-break front, macronutrient levels were high (surface nitrate $= 16.6 \, \mu$M, phosphate $= 0.35 \, \mu$M, silicate $= 4.0 \, \mu$M), associated with low phytoplankton biomass (<2 mg m^{-3}). This was due to mixing and advection associated with the MC flow and to grazing pressure at a transitional site between the MC and the high chlorophyll patch. Primary production rates (determined by the ^{14}C technique) ranged between 1.9 and 7.8 g C m^{-2} d^{-1}. Primary production was highest near $42°$S partly because of the elevated phytoplankton biomass, which consumed most of the nitrate and phosphate in surface waters in this region. These high primary production rates are comparable with maximal seasonal productivity at eastern boundary currents. The large bloom extent at the Patagonian shelf-break (approximately 55,000 km^2 patch of >2 mg m^{-3} chlorophyll), the associated primary production rates and diatom dominance indicate a potentially significant biological control of gases such as O_2 and CO_2 in surface layers. The main

* Corresponding author. Tel.: +55 53 32336510; fax: +55 53 32336601.
E-mail addresses: birfurg@hotmail.com, docvmtg@furg.br (V.M.T. Garcia), dfsgar@furg.br (C.A.E. Garcia), dfsmata@furg.br (M.M. Mata), pollery@hotmail.com (R.C. Pollery), apiola@hidro.gov.ar (A.R. Piola), Sergio.Signorini@nasa.gov (S.R. Signorini), charles.r.mcclain@nasa.gov (C.R. McClain), dir@noc.soton.ac.uk (M.D. Iglesias-Rodriguez).

factors favoring the development and maintenance of these blooms are nutrient supply from MC upwelling and water column stability. Other processes such as mixing or grazing play an important role in biomass modulation in the region.

1. Introduction

The Patagonian shelf off Argentina shows complex dynamic processes influenced by tides, the confluence of two western boundary currents (Brazil and Malvinas Currents), and freshwater discharge from the Rio de la Plata. Several oceanographic fronts can be identified in the shelf region associated with high chlorophyll concentrations (Acha et al., 2004; Bianchi et al., 2005; Carreto et al., 1995). At the shelf-break, the cooler and more saline waters of the Malvinas Current (MC), which is derived from the Antarctic Circumpolar Current, meet the subantarctic shelf waters producing a front with mild to weak density gradient (Martos and Piccolo, 1988). The cross-shelf-break temperature gradient is strongest in austral summer and autumn (Saraceno et al., 2004) and is also associated with enhanced chlorophyll concentration (Acha et al., 2004; Rivas et al., 2006; Romero et al., 2006). The frontal areas on the shelf and at the shelf-break are associated with intense ocean CO_2 uptake in late summer, with estimated mean seasonal fluxes of up to $-5.7 \, \text{mmol} \, CO_2 \, \text{m}^{-2} \, \text{d}^{-1}$ (Bianchi et al., 2005). Studies based on a large number of surface pCO_2 measurements and NCEP/NCAR wind data suggest that this area is a significant sink for atmospheric CO_2, with an important contribution from biological production (Takahashi et al., 2002). The high productivity of this region sustains stocks of several species of commercial fish and squid, which spawn and feed along the Patagonian shelf-break front, including the Argentine hake *Merlucius hubbsi* (Podestá, 1990), anchovy *Engraulis anchoita* (Berlotti et al., 1996), and the shortfin squid *Illex argentinus* (Berlotti et al., 1996). The intense fishing activities in this area have been depicted through remote sensing of global light-fishing (Rodhouse et al., 2001).

Recent studies based on both past (CZCS) and recent (SeaWiFS) ocean color sensors suggest that phytoplankton production has increased significantly over the past two decades in the southwestern Atlantic ocean, particularly in the Patagonian shelf region (Gregg et al., 2005). This trend has also been detected in 6 years of SeaWiFS data (Rivas et al., 2006). However, there is no published report of *in situ* data collected simultaneously with satellite records to validate ocean color algorithms for this region.

Along the Patagonian shelf-break front, consistent streaks of high chlorophyll (seen in Fig. 1) are observed during austral spring and summer, often being more than 1000 km long (Romero et al., 2006; Saraceno et al., 2005; Rivas, 2006). High phytoplankton biomass associated with the shelf-break front at 38–39°S was attributed to nutrient renewal by mixing on the slope, where the subantarctic waters of the MC are a source of macronutrients, especially nitrate (Carreto et al., 1995). Measurements of primary production during a dinoflagellate bloom near the shelf-break (at 39°S) showed values of $0.1–2.7 \, \text{g} \, C \, \text{m}^{-2} \, \text{d}^{-1}$ (Negri et al., 1992).

In satellite ocean color images, the chlorophyll patches associated with the shelf-break front show high blue reflectance, especially in mid summer, characteristic of coccolithophorid blooms (Brown and Podesta, 1997; Brown and Yoder, 1994). The seasonal variation of this high chlorophyll band (from $\sim$37 to 51°S) has recently been studied with a series of ocean color SeaWiFS images (Garcia et al., 2004; Rivas, 2006; Rivas et al., 2006; Romero et al., 2006; Saraceno et al., 2005). Apparently, this thermal front between the stratified subantarctic shelf waters and the cooler and vertically mixed water of the MC provides both light (on the stratified side) and nutrients (on the turbulent side) to sustain high phytoplankton biomass levels at the front during the warm season (spring and summer). However, both the phytoplankton biomass and community composition may differ substantially between the two seasons. The blooms begin in austral spring, probably dominated by diatoms, when chlorophyll-*a* concentration is maximum (Signorini et al., 2006), but in early austral summer (December, January), there is indication of a shift in the phytoplankton community, with dominance of calcite-producing phytoplankton and moderate chlorophyll concentration (Brown and Podesta, 1997; Brown and Yoder, 1994; Signorini et al., 2006).

Despite the ecological and biogeochemical relevance of the shelf-break front, to date there are only scarce *in situ* measurements of the phytoplankton community structure and primary production along the shelf-break front to confirm these seasonal patterns. Moreover, the possible physical and chemical mechanisms that drive and sustain the phytoplankton blooms are not fully understood.

Here we present results of a cruise carried out along the Patagonian shelf-break in November 2004, during the first field campaign of the PATagonian EXperiment (PATEX). The experiment was designed to determine the phytoplankton taxonomic composition, primary production rates and the main oceanographic, optical and biogeochemical features associated with shelf-break blooms in spring and summer. The main goals of the present work are to determine the phytoplankton community, biomass and primary production levels along the Patagonian shelf-break front in spring and to explore the associated physical, chemical and biological mechanisms.

2. Methods

2.1. Sampling

Nineteen oceanographic stations were sampled during 3–6 November 2004 in the vicinity of the Patagonia
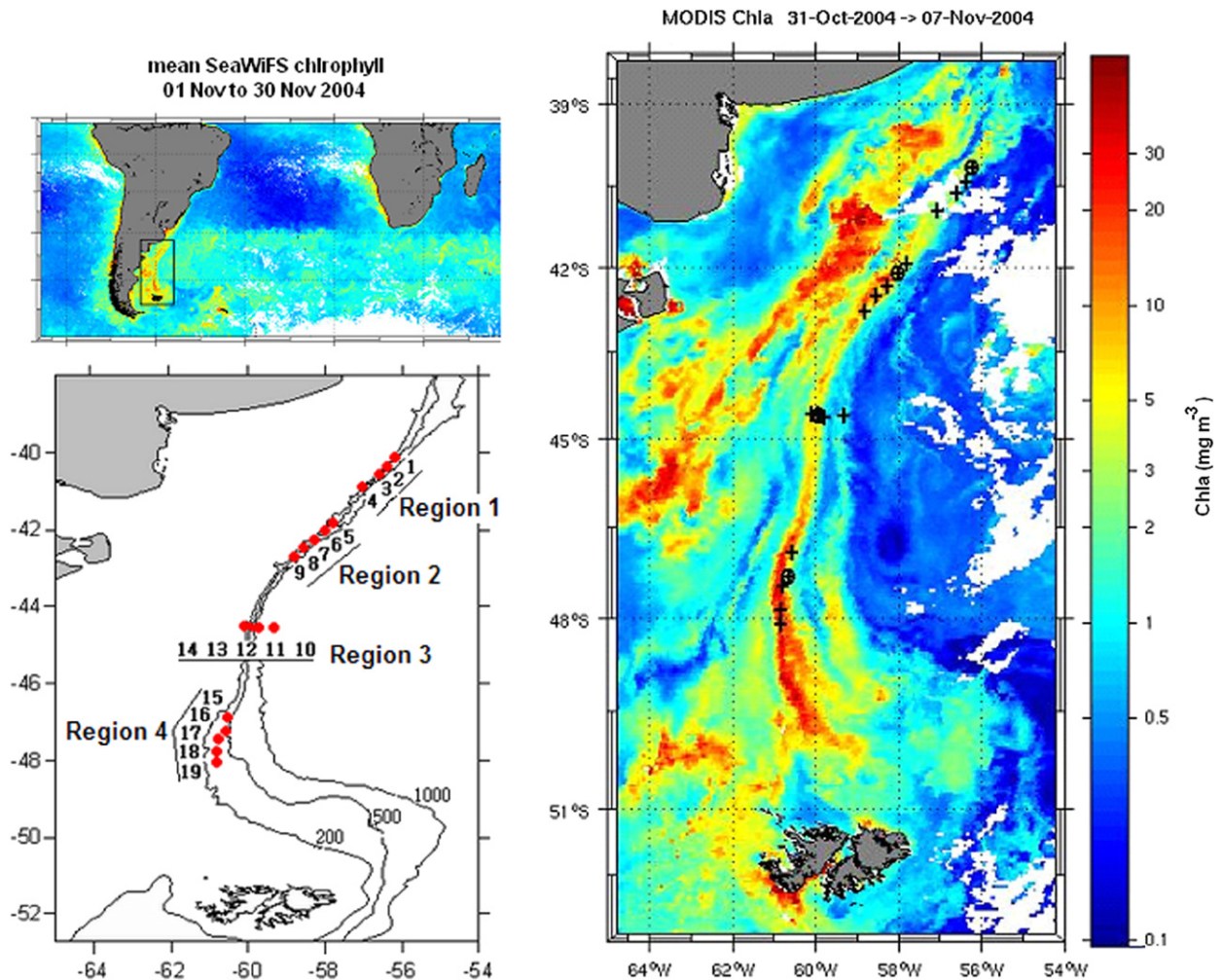
Fig. 1. Right panel: MODIS Aqua Chlorophyll image composite from 31 October to 07 November 2004, showing the sampling stations during the PATEX I cruise (3–6 November) along the high chlorophyll band at the Patagonian shelf-break. Four stations with a circle (Stns. 1, 6, 12 and 16) indicate the four sites where primary production was measured. The upper left side inset shows the study region on a monthly SeaWiFS chlorophyll composite (01–30 November 2004). The lower inset shows bathymetric lines and station numbers.

shelf-break (Fig. 1). Sampling was conducted during daytime, in groups of four or five stations, with the ship sailing southwards at night. Three transects were sampled along the shelf-break front (regions 1, 2 and 4), and one transect was sampled across the front, at 44°S (region 3).

Vertical profiles of temperature, salinity, dissolved oxygen and chlorophyll fluorescence (Seapoint® chlorophyll fluorometer) were taken with a SeaBird® 911+ Carrousel system. Water samples were collected from several depths using 5-l Niskin bottles for laboratory analysis of plankton and nutrients. Several water samples were stored and analyzed for salinity with a Guildline® 8400B Salinometer at the laboratory after the end of the cruise. The samples showed no significant drift in the temperature and conductivity from the sensors.

Vertical profiles of the photosynthetically active radiation (PAR) were taken at most stations by a LICOR® spherical quantum sensor. A LICOR® flat quantum sensor was placed on the ship's mast for monitoring of the incident PAR radiation, which was recorded on a data logger (LI-1400 model).

2.2. Phytoplankton identification

Samples for phytoplankton counting and identification, collected from the surface, were fixed with alkaline lugol's solution (Utermöhl, 1958) for later microscope examination. At the laboratory, 2–10 ml sub-samples were settled in Uthermöhl chambers and analyzed using a Zeiss® Axiovert inverted microscope, at $200 \times$, $400 \times$ and $1000 \times$ magnifications. For coccolithophorid identification, samples were gently filtered through *Isopore* filters mounted on top of Whatman® GF/C filters. Cell examination was made on a LEO 1450VP scanning electron microscope (SEM) at the National Oceanography Centre, Southampton.

2.3. Phytoplankton pigment analysis

Discrete samples for chlorophyll-*a* determination were collected from the surface and selected depths based on the fluorescence profile and filtered onto Whatman® GF/F filters, which were kept frozen in liquid nitrogen until analyzed. At the laboratory, the pigment was extracted in 90% acetone and fluorescence determined in a Turner Designs TD-700 fluorometer (previously calibrated with Sigma® chlorophyll-*a* standards), following the non-acidification method of Welschmeyer (1994). Water column integrated chlorophyll (mg m^{-2}) was calculated by fitting a Gauss curve to the discrete chlorophyll measurements (Platt et al., 1994) and integrating over depth to the 0.1% surface irradiance level.

2.4. Primary production measurements

Simulated *in situ* primary production measurements were carried out at four stations along the shelf-break by the ^{14}C technique (Steemann, 1952). Water samples were collected from 5 m depth (representing the mixed layer) and from chlorophyll subsurface peaks for $P \times I$ experiments at six irradiance levels (in triplicate). Sub-samples of 50 ml were dispensed in polystyrene flasks and inoculated with 10 μCi of ^{14}C-sodium bicarbonate. During incubation (4–6 h) irradiances in the sample flasks were equivalent to 100% (no mesh), 75%, 47%, 28%, 14%, 5.5% (and one dark treatment) of incident light. After incubation, samples were filtered through 25 mm Whatman GF/F filters and washed with the same volume of filtered seawater and these were kept frozen until laboratory analysis. Small (200 μl) sub-samples were taken from the sample flasks after inoculation to check for the added radioactivity. Sub-samples and filters were then processed following the procedure described by Parsons et al. (1984).

Photosynthetic parameters (P_{max}, alpha, beta) were estimated from the $P \times I$ measurements by fitting a model to the data (Platt et al., 1980). Water column production (mg C m^{-2} h^{-1}) was estimated by applying the photosynthetic parameters to irradiance values in the water column, based on PAR incident irradiance and attenuation coefficient. Daily primary productivity (mg C m^{-2} day^{-1}) was then calculated by integrating hourly production over the daylight hours, based on the surface incident PAR measurements.

2.5. Nutrient analyses

Water samples for dissolved inorganic nutrients (nitrate, nitrite, ammonium, phosphate and silicate) were collected at all stations from the surface and selected depths using Niskin bottles and filtered through cellulose acetate membrane filters. Nutrients were analyzed on board ship, following the processing recommendations in Strickland and Parsons (1972). Ammonium was measured by the method of Koroleff (1969) following modifications in Grasshoff et al. (1983) and absorbance readings at 630 nm. Nitrite and nitrate concentrations were measured

according to Strickland and Parsons (1972). Orthophosphate was measured by reaction with ammonium molybdate and absorption reading at 885 nm. Silicate in the form of reactive Si was measured according to Strickland and Parsons (1972) and correction for sea salt interference made following Aminot and Chaussepied (1983). Absorbance values for all nutrients were measured in a FEMTO® spectrophotometer.

2.6. Physical parameter calculations

The potential temperature and salinity data obtained from the CTD measurements were used to calculate potential density and the stability parameter (E). The latter, a measure of water column stability, is proportional to the buoyancy (or Brunt-Väisälä) frequency (N^2) and defined by:

$$N^2 = -\frac{g}{\rho}\frac{\partial \rho}{\partial z} \left(\text{rad}^2 \text{ s}^{-2}\right)$$

$$\text{leading to } E = \frac{N^2}{g} \left(10^{-8}\text{rad}^2 \text{ m}^{-1}\right),$$

where g is gravity and ρ is the water density. In this study, E was used to determine the vertical profile of water column stratification.

3. Results

3.1. Physical setting

The T/S diagram for all stations occupied during the cruise (Fig. 2A) shows the presence of subantarctic shelf waters (marked as shallow stations) and MC waters (mainly at Stn. 10). Stn. 11 represents a transition between those two water types. Temperature and salinity varied from 2.75 to 8.87 °C and from 32.13 to 34.39, respectively, in the sampled region. Apparently, bottom waters on the Patagonia outer shelf originate from the MC (see dashed circle in Fig. 2A). The upper column of MC subantarctic waters (Stn. 10) is colder (and more saline) than Patagonian shelf-break waters (Fig. 2A). The cross-shelf section collected in region 3 (Stns. 10–14; Fig. 2B) reveals the offshore isotherm shoaling associated with the MC axis. Note that the temperature profile at Stn. 10 (offshore) is distinct from the other stations in that transect, suggesting intense mixing and weaker vertical stratification in the upper 30 m of the water column.

3.2. Nutrient distribution at the shelf-break front

The distributions of dissolved inorganic nitrogen (DIN, comprising nitrate, nitrite and ammonium) and phosphate in the four sampling regions are shown in Fig. 3A. Surface nutrient values can be seen in Table 1. High values of DIN were observed below 50 m (>15 μM), decreasing sharply towards the surface (Fig. 3A). Exceptions were Stns. 10 and 11 (region 3), where the large stocks of nutrients in surface layers suggest they are not consumed by phytoplankton. Ammonium constituted an important fraction of dissolved inorganic nitrogen, indicating
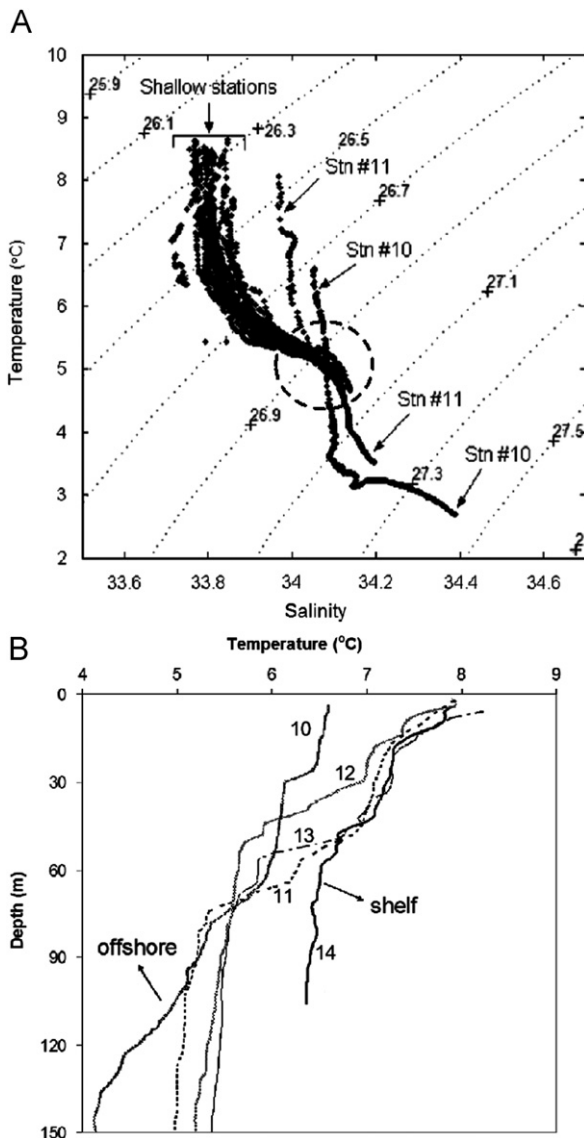
A

B

Fig. 2. (A) *T/S* diagrams (temperature, °C, and salinity) of all the cruise stations. *T/S* of Stns. 10 and 11 (eastern most stations at Region 3) are marked on the graph. (B) Upper layer vertical profiles of temperature at Stns. 14 (shelf) through 10 (offshore), of Region 3 (cross-shelf). Station numbers are marked on respective profiles.

significant recycling at the shelf-break front. Average surface ammonium fraction at the front (excluding Stns. 10, 11 and 14) was 13.5% and considering the upper 50 m decreased to 8.2%. However, overall ammonium concentration in the upper 50 m was not large (from 0.08 μM at surface, Stn. 19 to 0.87 μM at surface, Stn. 13). Phosphate in the upper 25 m was very low, with values <0.2 μM in surface waters (Fig. 3A). Distributions of silicate and density (sigma−θ) are shown in Fig. 3B. Si values at the surface varied from 0.9 μM (Stn. 13) to 3.9 μM (Stn. 10), increasing with depth, in a similar pattern as density.

The relationships between macronutrients and temperature are shown in Fig. 4. The close associations with temperature indicate that cold deep waters are a source of nutrients to the frontal system. Silicate was better related with temperature through an exponential function, indicating a steeper decrease of this nutrient towards the surface. This may reflect differences in uptake or recycling dynamics between nitrogen and silica in the water column. Ratios of Si:N were highly variable in the 0–50 m water column (mean 0.8 ± 0.93) but were consistently <0.5 between 50 and 500 m, confirming that the Subantarctic Water source is relatively Si-depleted, as has been shown for the ACC waters north of the Polar Front (e.g. Brzezinski et al., 2001; Pondaven et al., 1999).

High N:P ratios were observed in most samples (mean surface N:P = 44), away from the "Redfield ratio" of 16:1 (Redfield et al., 1963). These high N:P ratios, coupled with low observed phosphate levels, suggest that phosphorus could have limited phytoplankton growth at some sites. However, recent studies (Klausmeier et al., 2004; Arrigo, 2005) have shown that higher N:P ratios (>30) can be adequate to phytoplankton species that are able to sustain growth under resource limitation.

3.3. Chlorophyll-a, phytoplankton groups and primary production

Chlorophyll-*a* (equivalent to phytoplankton biomass) was particularly high in the upper 50 m (Fig. 5), with surface values ranging from 1.8 mg m^{-3} (Stn. 11) to 19.9 mg m^{-3} (Stn. 19). The lowest values (<2 mg m^{-3}) were measured at both Stns. 10 and 11, located at the cross-shelf-break transect in region 3. Chlorophyll distribution at this location shows a marked lateral gradient from Stn. 11 to Stn. 13, where the high biomass (>12 mg m^{-3}) is associated with the shelf-break front.

Chlorophyll concentration was positively correlated with dissolved oxygen saturation (Fig. 6A; $p < 0.001$), suggesting that the biological processes are important in gas exchange dynamics in the region. This correlation is also illustrated in Fig. 6B, where vertical profiles of fluorescence, dissolved oxygen and chlorophyll are plotted.

Fig. 7A shows the abundance of the main phytoplankton groups along the high chlorophyll band (excluding Stns. 10, 11 and 14). Total cell abundance closely followed chlorophyll concentration (thick black line in Fig. 7A). The phytoplankton community was numerically mainly comprised of small-size diatoms (2–10 μm), followed by nano-phyto-flagellates (<20 μm) and a small contribution of large dinoflagellates. Although the abundance of dino-flagellates was very small, their calculated carbon biomass exceeded that of the other groups (Souza and Garcia, in preparation). The diatom community was dominated by species of the genus *Thallasiosira*. Only a few cells of the coccolithophorid *Emiliania huxleyi* were detected among the phytoplankton community (Fig. 7B). The distribution of the main phytoplankton groups in region 3 is shown in Fig. 8. While diatoms were most abundant in the phytoplankton community associated with the shelf and shelf-break front, at Stn. 10, east of the front, the community was dominated by very small (2–5 μm)
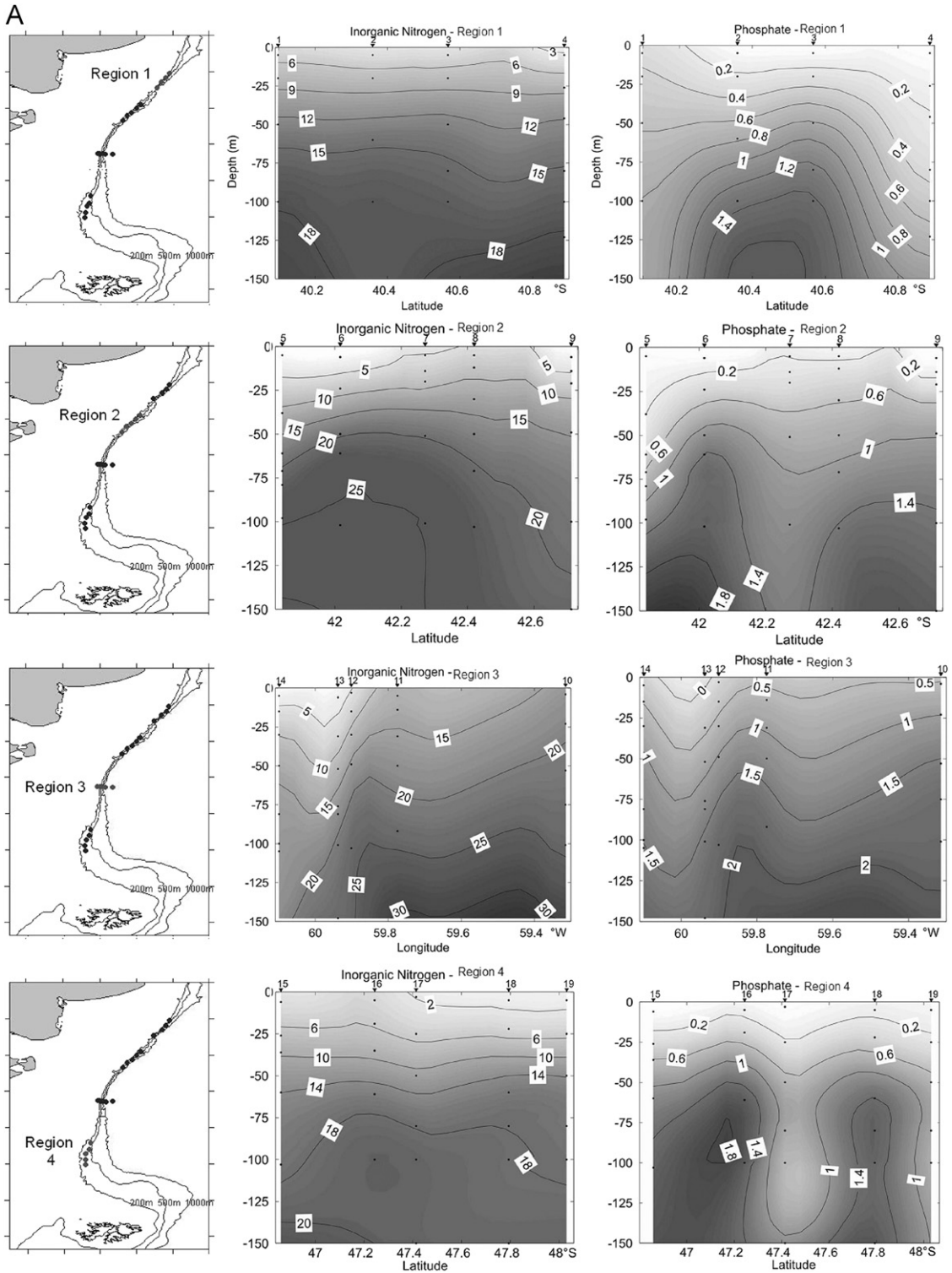
Fig. 3. (A) Left panels: Positions of stations in each sampling region at the Patagonian shelf-break. Middle and right panels: Water column distribution of dissolved inorganic nitrogen (nitrate+nitrite+ammonium), μM, and phosphate (μM), respectively, in the corresponding regions. Station numbers are marked on top of each graph. (B) Left panels: Positions of stations in each sampling region at the Patagonian shelf-break. Middle and right panels: Water column distribution of silicate (μM) and density (kg m^{-3}), respectively, in the corresponding regions. Station numbers are marked on top of each graph.
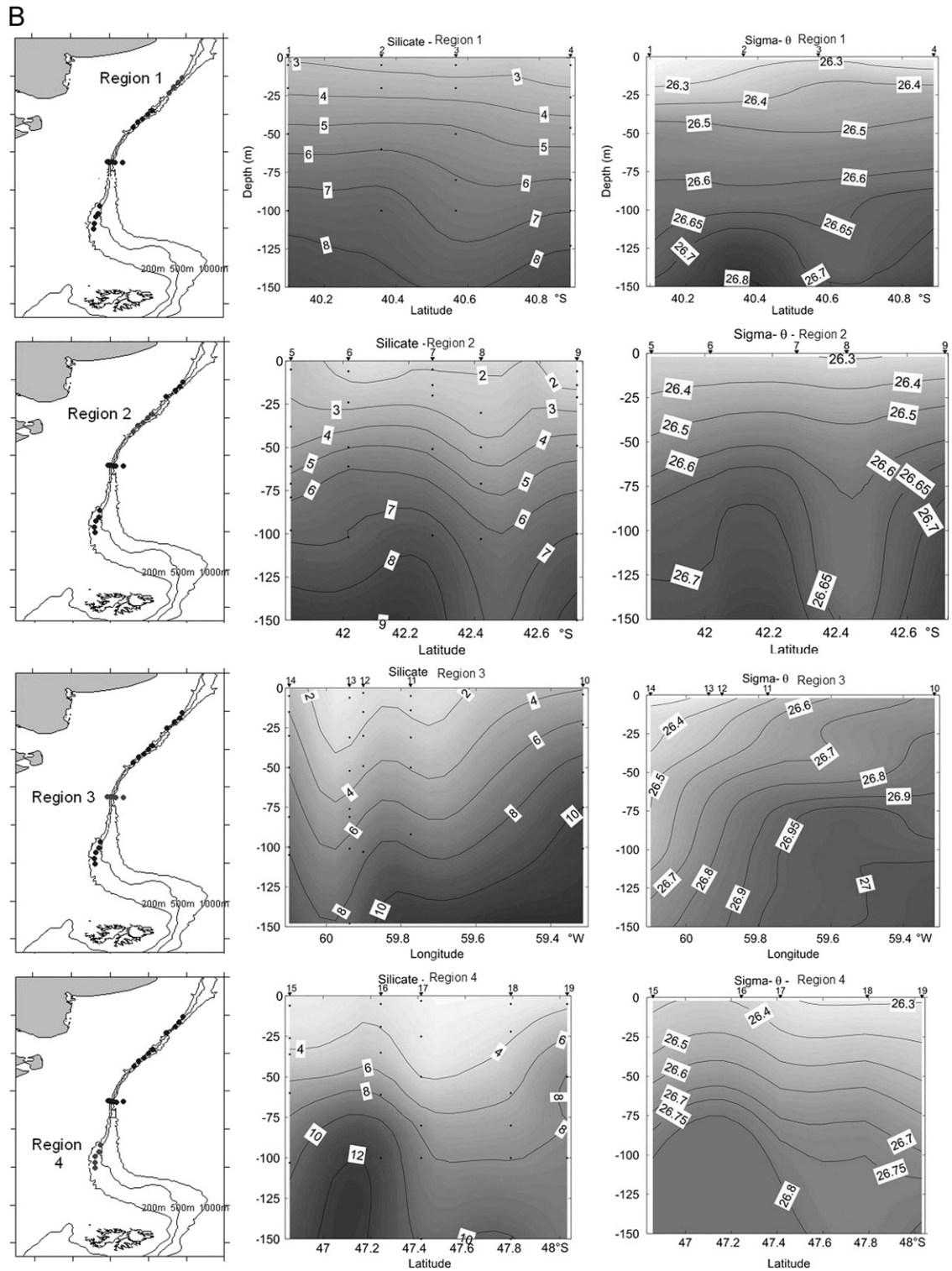
Fig. 3. (*Continued*)

phyto-flagellates, represented mainly by *Phaeocystis* cf. *antarctica*. Unfortunately, samples for phytoplankton counting were not collected at Stn. 11.

Primary production rates determined by the ^{14}C technique at four stations along the Patagonian shelf-break (see Fig. 1) are shown in Table 1, together with surface

Table 1
Values of water column integrated chlorophyll-*a* and primary production (at four stations) and surface water chemical properties at all stations along the Patagonian shelf-break in November 2004

Stn.	Day in November	Position	Surface NO$_3$ (μM)	Surface PO$_4$ (μM)	Surface SiO$_4$ (μM)	Surface Chl*a* (mg m^{-3})	Integrated Chl*a* (mg m^{-2})	Integrated primary production (g C m^{-2} d^{-1})
01	03	40.097°S, 56.200°W	6.08	0.30	3.37	3.23	335	3.24
02	03	40.358°S, 56.370°W	3.82	UDL	2.62	6.43	306	–
03	03	40.567°S, 56.582°W	3.70	UDL	2.20	11.29	597	–
04	03	40.887°S, 57.053°W	1.01	UDL	1.93	11.28	672	–
05	04	41.840°S, 57.777°W	0.82	0.12	3.16	12.40	1074	–
06	04	42.015°S, 57.990°W	0.65	0.02	1.50	13.63	893	7.79
07	04	42.272°S, 58.272°W	3.50	0.25	1.87	9.11	767	–
08	04	42.418°S, 58.543°W	4.68	0.07	1.61	8.57	681	–
09	04	42.712°S, 58.787°W	1.05	UDL	1.34	4.71	829	–
10	05	44.540°S, 59.317°W	16.22	0.35	3.96	2.00	90.4	–
11	05	44.558°S, 59.773°W	12.90	0.40	1.29	1.81	108	–
12	05	44.538°S, 59.900°W	3.87	0.07	1.07	10.67	358	1.96
13	05	44.520°S, 59.937°W	2.55	0.07	0.91	12.99	754	–
14	05	44.517°S, 60.098°W	0.80	0.15	3.21	7.94	614	–
15	06	46.858°S, 60.537°W	2.57	0.02	3.00	8.10	961	–
16	06	47.243°S, 60.623°W	4.21	0.12	3.27	5.93	378	2.08
17	06	47.413°S, 60.778°W	1.44	0.02	2.57	12.53	955	–
18	06	47.792°S, 60.838°W	0.70	0.10	2.95	16.49	727	–
19	06	48.030°S, 60.827°W	0.75	0.07	2.57	19.93	815	–
Average			3.75	0.11	2.34	9.49	627	3.77

Mean surface incident irradiance over the period of primary production experiments were 1323, 1407, 1255 and 1760 μmol m^{-2} s^{-1} at Stns. 01, 06, 12 and 16, respectively (UDL: under detection limit).

nutrient levels. Integrated primary production rates varied from 1.96 g C m^{-2} d^{-1} at Stn. 12 to 7.79 g C m^{-2} d^{-1} at Stn. 6. At the latter station, production was particularly high, partly because of the elevated phytoplankton biomass (893 mg chl*a* m^{-2}, as compared to 358 mg chl*a* m^{-2} at Stn. 12). Phytoplankton growth at this location must have consumed most nutrients in surface waters, resulting in the lowest nitrate levels (0.65 μM) (Table 1).

4. Discussion

Several recent studies have described the seasonal cycle of phytoplankton concentration at the Patagonian shelf-break from analysis of ocean color sensors (Garcia et al., 2004; Rivas, 2006; Rivas et al., 2006; Romero et al., 2006; Saraceno et al., 2005; Signorini et al., 2006). Although the high chlorophyll band presents important interannual variability in the bloom intensity (mean chlorophyll concentration) (Signorini et al., 2006), its location is stable (Romero et al., 2006) because the shelf-break front is bottom trapped (Saraceno et al., 2004). Due to the high latitudinal range of the frontal region, there is a marked difference in timing of the spring bloom initiation (Rivas et al., 2006), mainly following the north–south progression of water column stabilization triggered by changes in the surface heat fluxes. On average, while in the northern area (39–40°S) the blooms start in mid August (Rivas et al., 2006; Saraceno et al., 2005) further south (50–55°S) the blooms begin in September (Rivas et al., 2006). According to these investigations, peaks in chlorophyll over the shelf-break appear in October–November. Therefore, the timing of our cruise (beginning of November) likely represents the peak in phytoplankton biomass in the region, especially in the southern area.
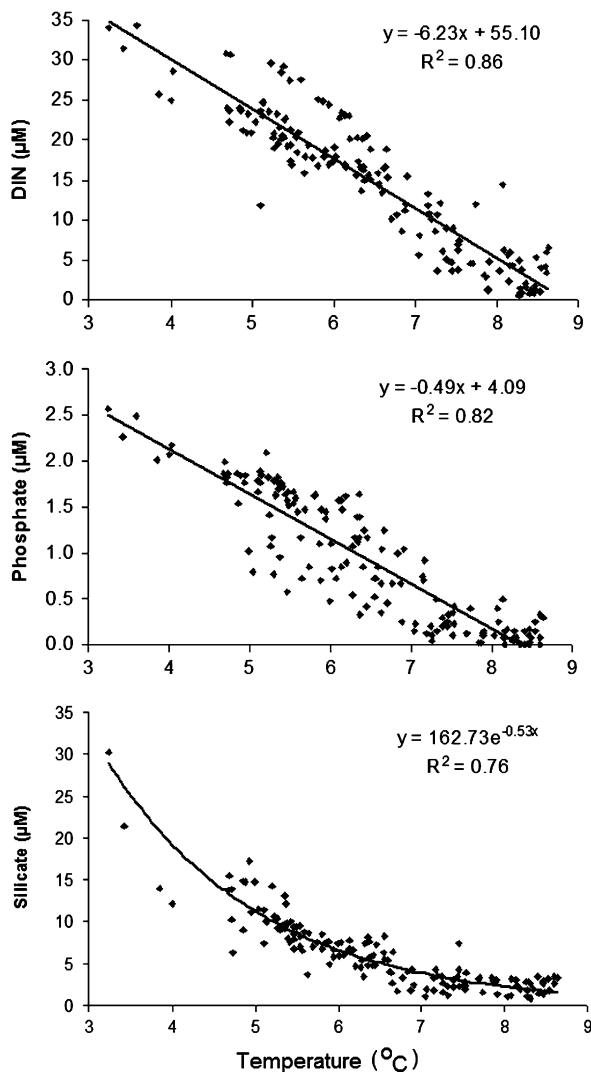
Fig. 4. Relationship between water temperature and macronutrients at the Patagonian shelf-break: dissolved inorganic nitrogen, DIN (nitrate+nitrite+ammonium) (top), phosphate (middle), and silicate (bottom).

4.1. Role of macro- and micro-nutrients during the shelf-break spring bloom

Nutrient supply at the shelf-break front is probably associated with the convergence flow and bottom friction, generating a pressure gradient along the shelf, resulting in upwelling along the front (Matano and Palma, 2008). Upwelling processes associated with shelf-break fronts are also observed in the North Atlantic (e.g. Loder et al., 1998; Allen et al., 2005), although the mechanisms leading to upwelling along the front can be different (Matano and Palma, 2008). It has also been suggested that the topography of the Patagonian shelf-break promotes mesoscale activity and generation of eddies which, in turn, supply nutrients to maintain the phytoplankton blooms (Longhurst, 1998). In this work, the arrangement of density isolines in region 3 (Fig. 3B) does suggest

upwelling occurred during our field sampling. In addition, the nutrient distributions at that transect (Fig. 3A and B) and the strong relationship between temperature and nutrients (Fig. 4) are also an indication of upwelling associated with MC subsurface waters. Similar cross-shelf-break structures at other latitudes have been reported by Piola and Gordon (1989), Peterson and Whitworth (1989) and Romero et al. (2006).

In surface waters, nutrient levels closely responded to phytoplankton biomass concentration, as seen in the inverse relationship between dissolved inorganic nitrogen (DIN) and chlorophyll-*a* (Fig. 9). The highest nutrient levels (Stns. 10 and 11) are associated with the lowest chlorophyll concentration. The inverse chlorophyll-*a* versus nutrient relationship leads to the strong horizontal gradient in near-surface DIN, observed in region 3, varying from 16.6 μM at Stn. 10 (offshore) to 0.99 μM at Stn. 14 (shelf). A similar nitrate gradient from coastal waters ($<2\,\mu$M) to the shelf-break ($>20\,\mu$M) was found by Carreto et al. (1995) at ~39°S in October/November 1987 and 1988. Macronutrients are apparently supplied by upwelling, while phytoplankton growth tightly controls the nutrient levels at the Patagonian shelf-break front. Processes associated with the low chlorophyll at both Stns. 10 and 11 will be addressed in the next sections.

In addition to macronutrients, iron availability may also play an important role in determining phytoplankton growth at the shelf-break. The surface waters of the MC are probably Fe-depleted, since the upper layers of the Antarctic Circumpolar Current are known to be iron poor (Loscher et al., 1997). Although there have been indications of an enhanced supply of trace metals by atmospheric dust input along the Patagonian coast (Erickson et al., 2003; Gaiero et al., 2003; Gasso and Stein, 2007), bio-availability of iron has not yet been determined in waters of the shelf-break front, which is located approximately 200–400 km from shore. Therefore, metal upwelling along the front cannot be ruled out as an important iron source to the bloom, which would sharply decrease towards the open ocean. In addition, shelf waters might also be an important source of iron in this region. For instance, further south, at a shallow shelf site, east of Malvinas Island, enhanced iron concentrations (up to 6 nM) were found both in surface waters and near the sediments (Bowie et al., 2002). Strong tidal mixing described for the region (Palma et al., 2004) and sediment ressuspension probably enhance Fe concentration in the shelf waters, providing an additional supply of this element to the shelf-break region. In this work, an indication of this process is shown by the distribution of silicate in the cross-shelf transect (Fig. 10), where higher levels of Si are associated with lower salinity, mid-shelf waters. This feature has been consistently observed during two other spring cruises to the region (R. Pollery, personal communication). Therefore, it is reasonable to suggest that shelf waters can also be an important source of metals to the shelf-break.

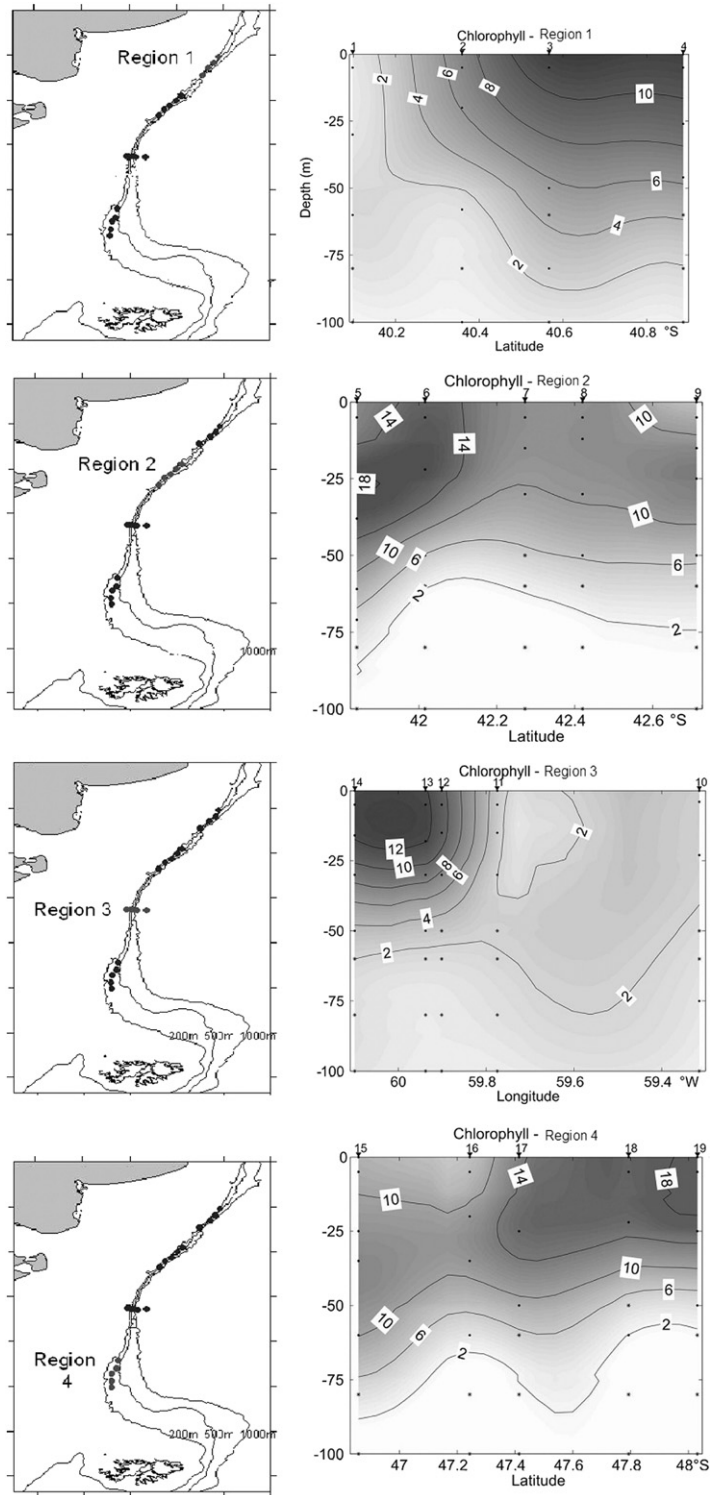Recent field studies along the Patos-Mirim lagoon system (30.5–32.5°S) (Windom et al., 2006) have

Fig. 5. Vertical distribution of chlorophyll-*a* (mg m^{-3}) in the four regions at the shelf-break front, shown on the left panels (3–6 November 2004).

suggested that submarine ground water discharge can be an important source of dissolved iron to the South Atlantic Ocean. It is suggested that the iron flux from these lagoons could be transported by the Brazil Current and reach the waters of the Brazil-Malvinas Confluence, including the shelf-break region south of 38°S.

In summary, we propose that nutrient supply for maintaining phytoplankton blooms in the study region,
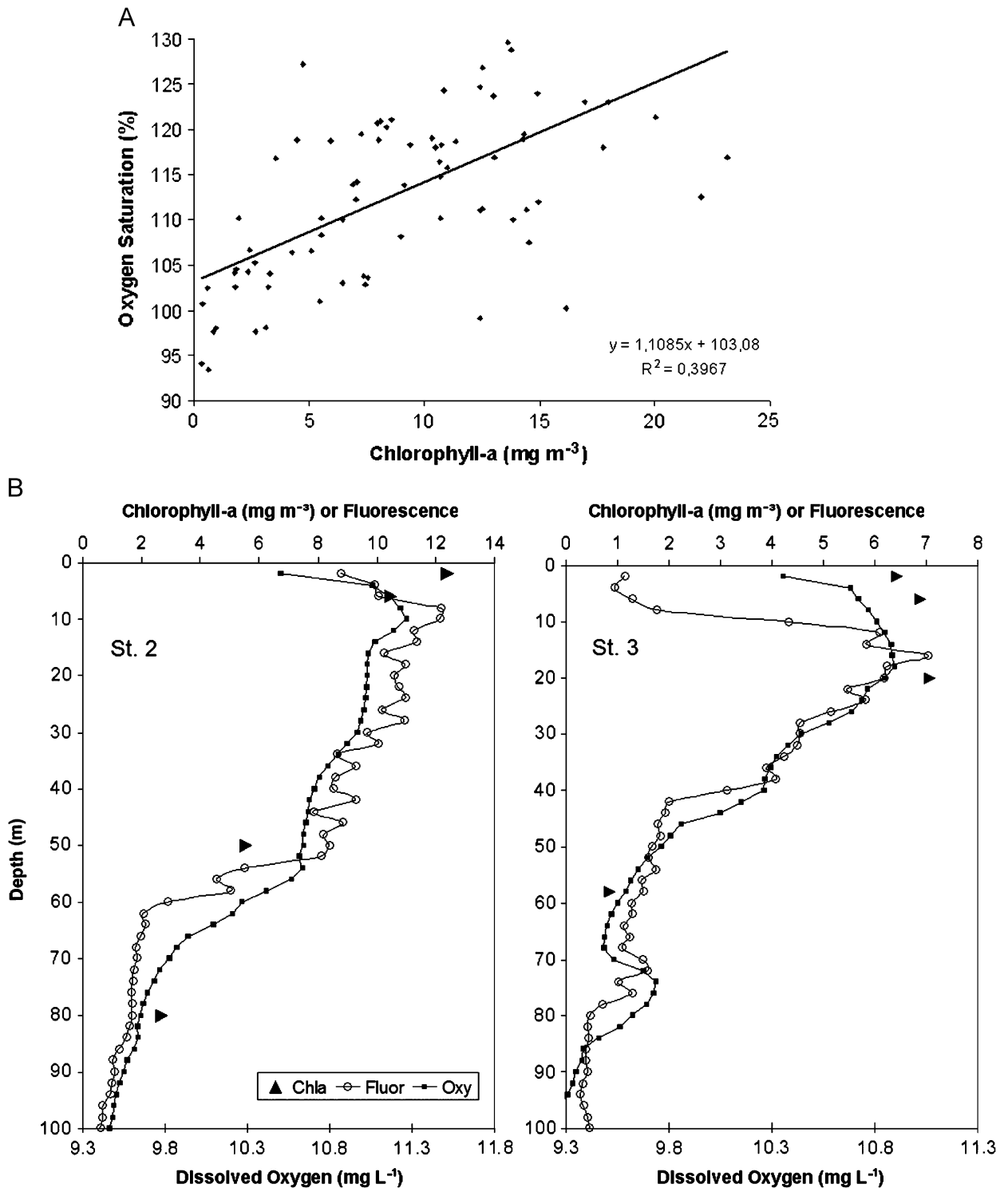
Fig. 6. (A) Relationship between oxygen saturation (%) and chlorophyll-*a* (*N* = 79). (B) Vertical profiles of dissolved oxygen, mg l^{-1} (squares), fluorescence, relative units (dots) and measured chlorophyll-*a*, mg m^{-3} (triangles) at Stn. 2 (left) and Stn. 3 (right). The fluorometer readings were scaled (internal calibration) to approximately match chlorophyll units.

particularly in spring, is provided by a combination of macronutrient availability from the rich MC, enhanced by upwelling along the front, and micronutrient (mainly iron), potentially supplied from four sources: upwelling, shallow shelf water, dust deposition and ground water from remote regions.
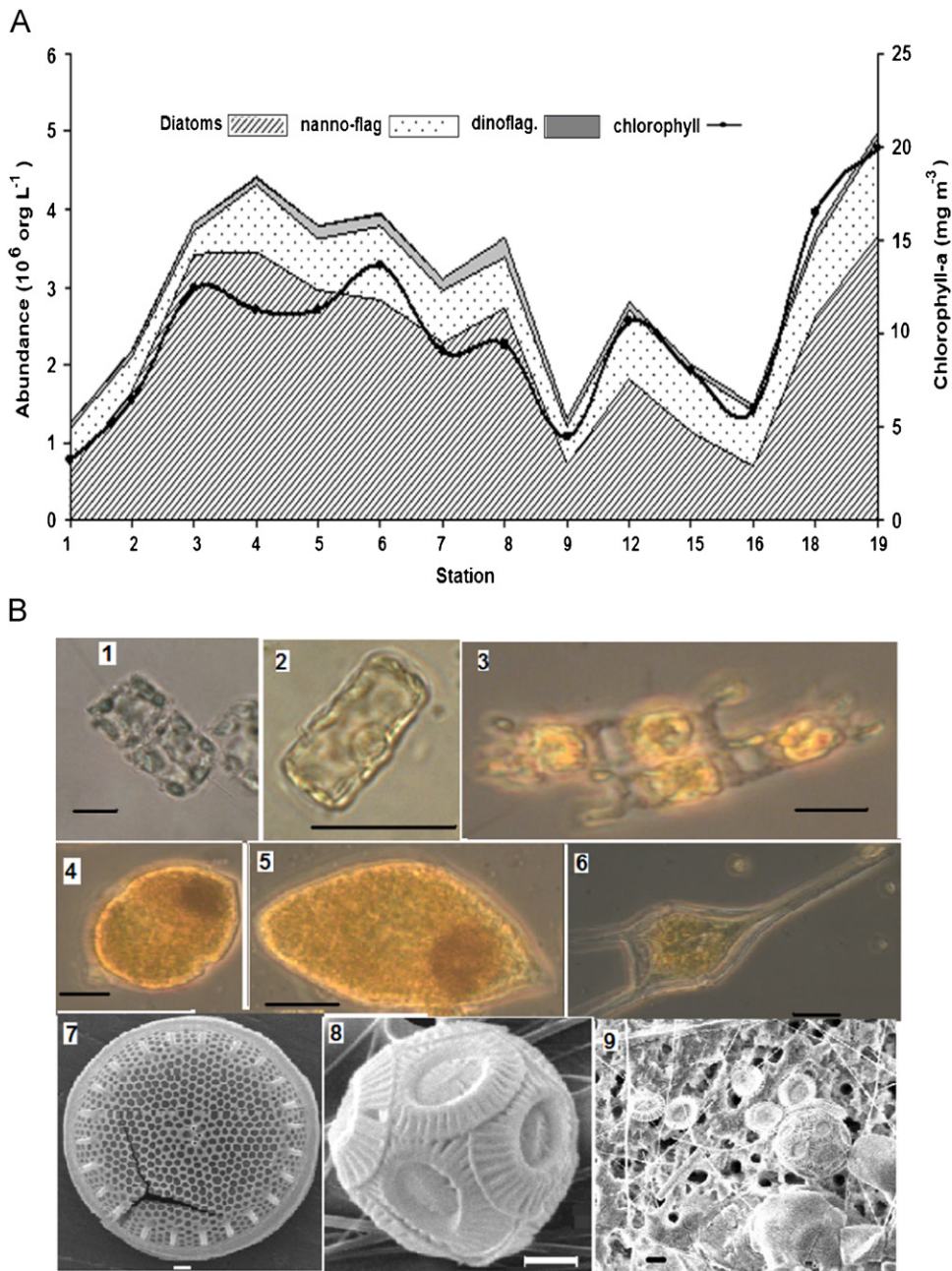
Fig. 7. (A) Surface chlorophyll-*a* (thick line) and abundance (10⁶ organisms l⁻¹) of main phytoplankton groups (diatoms, nanoflagellates and dinoflagellates) along the high chlorophyll band. (B) Photomicrographs of diatoms (1–3, light microscopy), dinoflagellates (4–6, light microscopy) diatoms (7, scanning electron microscope—SEM) and *Emiliania huxleyi* (8 and 9, SEM). 1: *Thallasiosira* sp.; 2: *Thallasiosira* cf. *weissflogii*; 3: *Eucampia* sp.; 4: *Gymnodinium* sp.; 5: *Gyrodinium* sp.; 6: *Ceratium* sp.; 7: *Thallasiosira* cf. *australis*; 8 and 9: *Emiliania huxleyi*. Scale bars are 10 μm (1–6) and 1 μm (7–9).

4.2. Water column stability

Physical factors, such as water column stability, probably play an important role in sustaining the phytoplankton cells in the euphotic layer along the shelf-break front, as previously suggested (Podestá, 1990). The onset of vertical stability is important for triggering spring blooms in temperate latitudes, when nutrients are available from the previous winter, but light is limiting by deep mixed layers (Sverdrup, 1953). However, strong and persistent stability, especially in summer, has a negative impact on phytoplankton growth because it acts as a barrier for upward nutrient input from below the nutricline to the nutrient-exhausted surface layers. At almost all stations sampled in this study, the water column was well stratified (mean stability index between 0 and 50 m
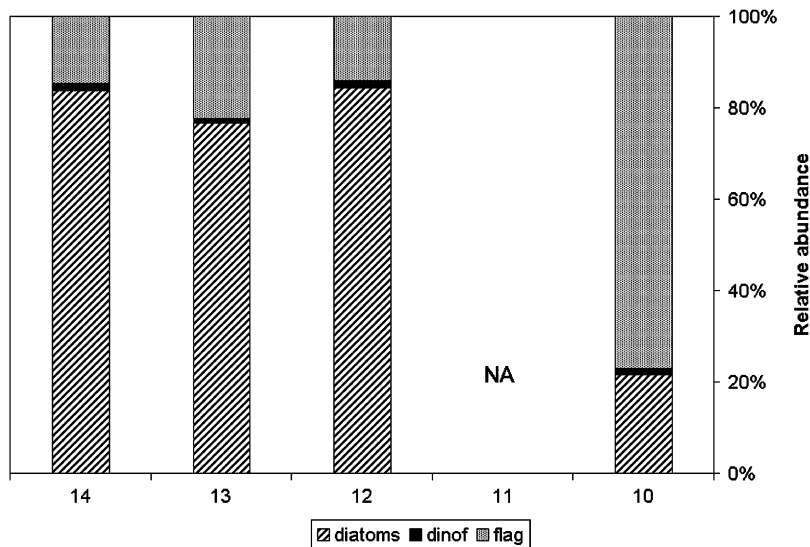
Fig. 8. Relative abundance in terms of cell numbers of phytoplankton groups in Region 3. Diat: diatoms; Dinof: dinoflagellates; Flag: nano-flagellates. Note the dominance of nano flagellates (mainly *Phaeocystis* sp.) at Stn. 10, associated with low chlorophyll values. NA: data not available at Stn. 11.
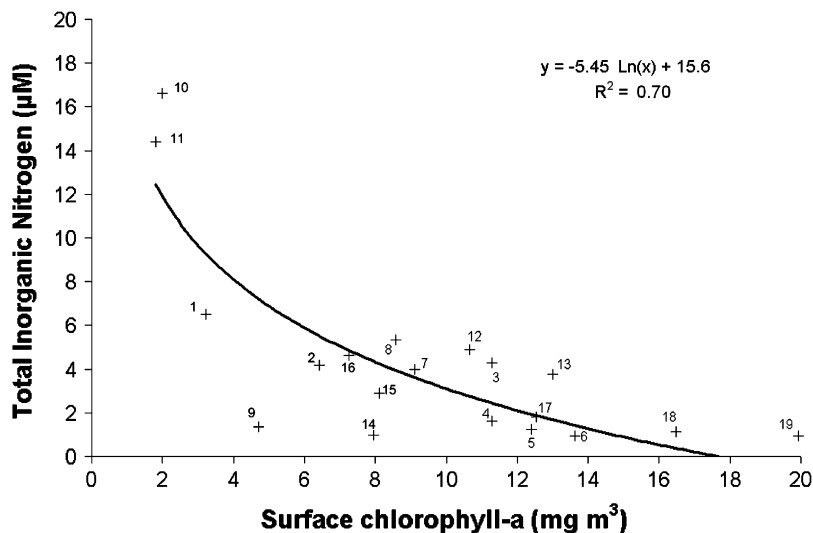

Fig. 9. Relationship between surface dissolved inorganic nitrogen (μM) and chlorophyll-*a* (mg m^{-3}) at all stations in the study region.

was from 220×10^{-8} to 740×10^{-8} rad^2 m^{-1}). An exception was Stn. 10 (most offshore station) with a value of <100 rad^2 m$^{-1} \times 10^{-8}$. This could partially explain the low chlorophyll found at this site. Fig. 11 shows the stability index and surface chlorophyll-*a* along the cross-shelf transect (region 3). Surface chlorophyll is highest over more stable waters (Stns. 12 and 13), implying that light could have been a limiting factor within the more turbulent MC waters (Stn. 10). This is in agreement with the dominance of the genus *Phaeocystis* at this station, which has been suggested to have a competitive advantage over diatoms under high-nutrient, low-light and deep-mixing conditions (Cota et al., 1994; Hegarty and Villareal, 1998; Moisan and Mitchell, 1999).

Another factor associated with the transport dynamics of the western boundary current is loss of phytoplankton cells by advection, particularly at Stns. 10 and 11. During sampling of those two stations, the vessel drifted north-eastward at >3 knots ($\sim$150 cm s^{-1}), which indicates a high-velocity jet, capable of "washing-away" phytoplankton cells downstream.

4.3. Possible grazing control on biomass levels

Apart from chemical and physical forcing on phytoplankton biomass and production, biological processes such as grazing pressure can play an important role in controlling biomass accumulations. Therefore, an
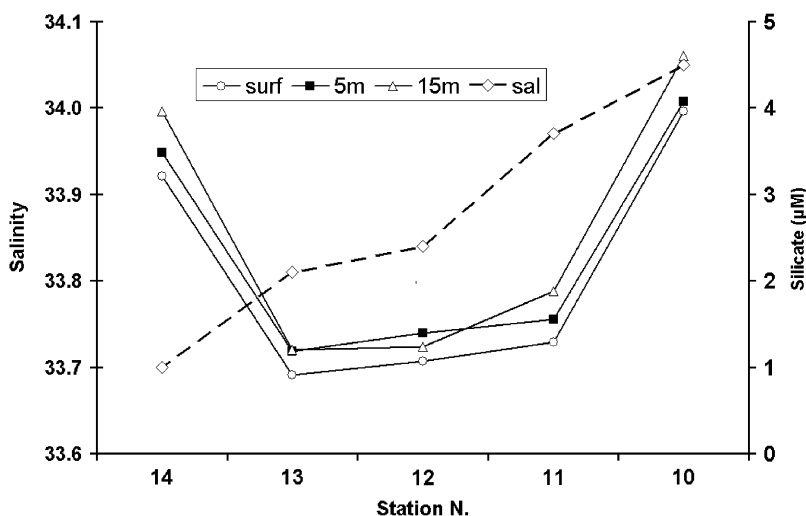
Fig. 10. Surface salinity (dashed line) and silicate concentration (μM) at the surface (circles), 5 m (filled square) and 15 m (triangle) in region 3 (Stns. 10–14).
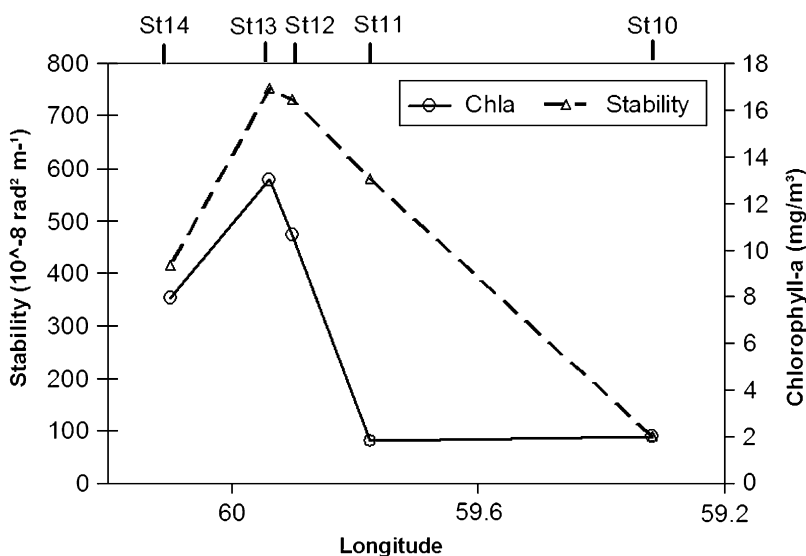

Fig. 11. Surface chlorophyll-a (circle+line) and mean water stability (E) in the top 50 m ($10^{-8}\,rad^2\,m^{-1}$) (triangle+dashed line) across the shelf-break (region 3).

alternative explanation for the low phytoplankton bio-mass found particularly at Stn. 11, where macronutrients are available in a stratified water column, is grazing pressure. This hypothesis is supported by the vertical distributions of macronutrients at this site (Fig. 12). An indication of strong grazing pressure at Stn. 11 is the distinctly higher concentrations of ammonium (Fig. 12A), a common excretion product of zooplankton. In addition, silicate concentrations at Stn. 11 are not distinct from those at the other stations along the shelf-break (Fig. 12B), indicating a similar level of utilization of this nutrient, and implying previous diatom growth. Unfortunately, confir-mation of the phytoplankton assemblage could not be made at this particular station, as no samples were available. The low Si concentration at Stn. 11 is in contrast

with that at Stn. 10, which stands out with the highest Si levels. Therefore, both Stns. 10 and 11 presented relatively low phytoplankton biomass ($<2\,mg\,m^{-3}$), but Stn. 11 showed an apparent previous Si utilization. These low silicate concentrations at Stn. 11 (1.3 μM at surface) were in contrast with high nitrate levels (surface DIN = 14.4 μM), a condition similar to that described for silicate controlled environments (Dugdale et al., 1995). This "silica pump" condition is driven by both a faster sinking and a slower recycling rate of Si (particularly in cold waters) as compared to nitrogen. This process is particularly en-hanced by grazing, whereby Si-enriched zooplankton fecal pellets increase silicon sinking rates, resulting in rapid loss of silicate from the euphotic layer, while nitrogen is regenerated faster in the grazing cycle (Dugdale et al.,
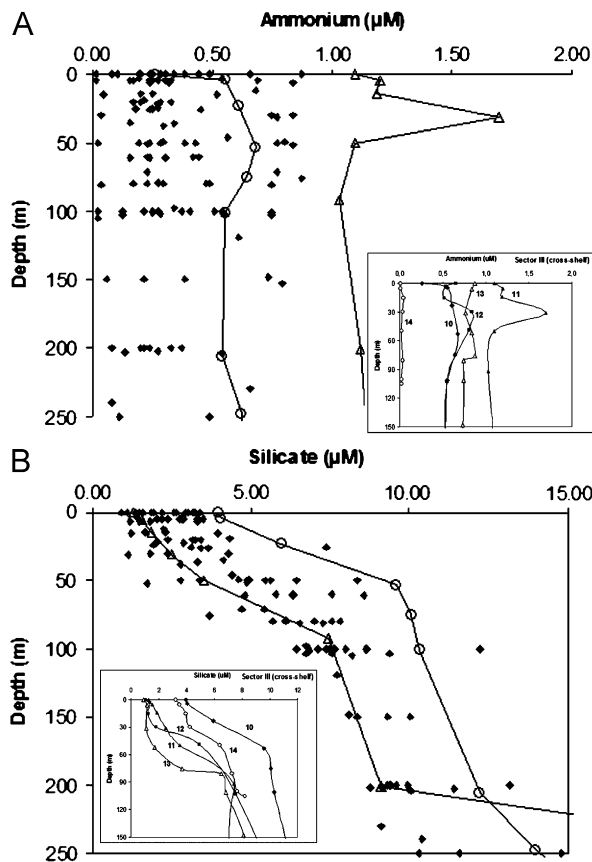
A

B

Fig. 12. Vertical profiles of ammonium (A) and silicate (B) at all cruise stations. Profiles of Stn. 10 (line+circles) and 11 (line+triangles) are highlighted. The insets show vertical profiles of the respective nutrients in region 3 (cross-shelf).

1995; Pondaven et al., 1999). The higher levels of ammonium generated in the process are a known preferable nitrogen source for phytoplankton, leading to accumulation of nitrate in the euphotic zone, as observed in this study. Therefore, at least some areas of the study region (and based on the generally low Si:N ratios) seem to function as a "silica pump", as observed at Stn. 11.

4.4. The phytoplankton community and primary production rates

The seasonal dynamics of phytoplankton groups in the region have been studied based on a time-series of SeaWiFS chlorophyll (OC4v4) and calcite concentrations (Signorini et al., 2006). The study suggests that in December coccolithophorids begin to dominate the water spectral signature at the shelf-break, after the spring diatom blooms. Data from the present work confirm the important role of diatoms in the phytoplankton community at the Patagonian shelf-break in spring, associated with high chlorophyll-a concentrations (2–20 mg m^{-3} at surface). However, as stated above, dinoflagellates were also important components of the biomass because of their generally greater size. Although the dynamics of

phytoplankton succession cannot be depicted from this work, the presence of fast growing small-size diatoms, the relative importance of large dinoflagellates and the low nutrient levels in the surface layers indicate an early to intermediate stage in succession (Margalef, 1962). Low cell densities of the coccolithophorid E. huxleyi were found among the dominating centric diatoms and flagellates. This small E. huxleyi population likely represents the inoculum for the subsequent coccolithophorid bloom development, as suggested in ocean color studies (e.g. Brown and Podestá, 1997; Signorini et al., 2006). In fact, the presence of coccolithophorids in early summer has recently been confirmed by in situ surveys carried out in January 2008 over a large patch of high reflectance located over the mid shelf (Garcia, VMT, in preparation).

These two types of communities (diatoms and cocco-lithophorids) represent different key functional groups of phytoplankton (Doney, 1999; Moore et al., 2002) and therefore play different roles in the food web structure and in the air–sea CO_2 exchange dynamics. While diatoms are normally associated with high production rates and elevated organic matter export flux (Buesseler, 1998; Sarthou et al., 2005), coccolithophorids can have an impact on CO_2 partial pressure in surface waters, by increasing this gas during $CaCO_3$ platelet formation (Holligan et al., 1993; Rost and Riebesell, 2004). Therefore, the alternation of dominance between the two groups in different seasons may result in significant changes in the CO_2 exchange dynamics in the region.

Primary production rates measured in this work varied from approximately 2–8 g C m^{-2} d^{-1}. The high magnitudes of photosynthesis caused dissolved oxygen to vary closely with phytoplankton biomass, as seen in Fig. 6. Rates of primary production during a dinoflagellate bloom in the vicinity of the shelf-break at 39°S were in the range 0.1–2.7 g C m^{-2} d^{-1} (Negri et al., 1992), somewhat lower than the values found in the present work. The high primary production rates in the present work are comparable with maximal seasonal productivity at eastern boundary current systems such as California, Peru-Chile (Humboldt), Canary and Benguela Currents. Large-scale primary production in those systems has been estimated between 2 and 6 g C m^{-2} d^{-1} (Carr and Kearns, 2003), similar to those found in this work.

The large bloom extent at the Patagonian shelf-break (approximately 55,000 km^2 patch of >2 mg m^{-3} chloro-phyll patch in November 2004) and the associated primary production rates may significantly impact ocean carbon uptake in the region. In fact, high sea–air partial pressure differences (Δp CO_2) into the ocean (maximum −110 μatm) have been found for this region in late summer (Bianchi et al., 2005). Recent Δp CO_2 estimates at the shelf-break between 39 and 50°S based on several cruises conducted in spring range between −40 and −200 μatm (Bianchi et al., 2008). Similarly, measurements of CO_2 fluxes along the same cruise track as the present work, in spring 2006, have also shown a conspicuous negative Δp CO_2 flux (−56.2 to −150 μatm) associated with the shelf-break bloom (Ito et al., in preparation). Furthermore, CO_2 fluxes on the Patagonian shelf were found to be well related to chlorophyll levels when the

phytoplankton community is dominated by diatoms (Schloss et al., 2007), as opposed to dominance by nano-flagellates. Therefore, data on biomass, primary production and community composition (dominance by diatoms) in the present study suggest that biological activity play a significant role in CO_2 dynamics in the region.

Results of the present work have shown that the spring phytoplankton blooms at the Patagonia shelf-break are associated with high primary production rates, comparable with very productive areas of the world oceans. The blooms are sustained by nutrient supply from the MC upwelling and are maintained in the upper layers (mainly above 50 m) by vertical stability. The elevated biomass levels ($2–17\,mg\,m^{-3}$ surface chlorophyll) are associated mainly with diatoms and dinoflagellates and apparently controlled by mixing and grazing pressure.

Acknowledgments

References

Acha, E.M., Mianzan, H.W., Guerrero, R.A., Favero, M., Bava, J., 2004. Marine fronts at the continental shelves of austral South America Physical and ecological processes. Journal of Marine Systems 44 (1/2), 83–105.

Allen, J.T., et al., 2005. Diatom carbon export enhanced by silicate upwelling in the northeast Atlantic. Nature 437 (7059), 728–732.

Aminot, A., Chaussepied, J., 1983. Manuel des Analyses Chimiques en Milieu Marin. C.N.E.X.O., Brest, 230pp.

Arrigo, K.R., 2005. Marine microorganisms and global nutrient cycles. Nature 437, 349–355.

Bertolotti, M.I., Brunetti, N.E., Carreto, J.I., Prenski, L.B., Sanchez, R.P., 1996. Influence of shelf-break fronts on shellfish and fish stocks off Argentina. International Council for the Exploration of the Sea, Copenhagen, C.M. 1996/S, 41pp.

Bianchi, A.A., et al., 2005. Vertical stratification and air–sea CO_2 fluxes in the Patagonian shelf. Journal of Geophysical Research—Oceans 110, C07003.

Bianchi, A.A., et al., 2008. Annual balance and seasonal variability of sea–air CO_2 fluxes in the Patagonia Sea: their relationship with fronts and chlorophyll distribution. Journal of Geophysical Research, under revision.

Bowie, A.R., Whitworth, D.J., Achterberg, E.P., Mantoura, R.F.C., Worsfold, P.J., 2002. Biogeochemistry of Fe and other trace elements (Al, Co, Ni) in the upper Atlantic Ocean. Deep-Sea Research Part I—Oceano-graphic Research Papers 49 (4), 605–636.

Brown, C.W., Podesta, G.P., 1997. Remote sensing of coccolithophore blooms in the western South Atlantic Ocean. Remote Sensing of Environment 60 (1), 83–91.

Brown, C.W., Yoder, J.A., 1994. Coccolithophorid blooms in the global ocean. Journal of Geophysical Research—Oceans 99 (C4), 7467–7482.

Brzezinski, M.A., Nelson, D.M., Franck, V.M., Sigmon, D.E., 2001. Silicon dynamics within an intense open-ocean diatom bloom in the Pacific sector of the Southern Ocean. Deep-Sea Research Part II—Topical Studies in Oceanography 48, 3997–4018.

Buesseler, K.O., 1998. The decoupling of production and particulate export in the surface ocean. Global Biogeochemical Cycles 12 (2), 297–310.

Carr, M.E., Kearns, E.J., 2003. Production regimes in four Eastern Boundary Current systems. Deep-Sea Research Part II—Topical Studies in Oceanography 50, 3199–3221.

Carreto, J.I., Lutz, V.A., Carignan, M.O., Colleoni, A.D.C., Demarco, S.G., 1995. Hydrography and chlorophyll-*a* in a transect from the coast to the shelf-break in the Argentinian Sea. Continental Shelf Research 15, 315–336.

Cota, G.F., Smith, W.O., Mitchell, B.G., 1994. Photosynthesis of Phaeocystis in the Greenland Sea. Limnology and Oceanography 39 (4), 948–953.

Doney, S.C., 1999. Major challenges confronting marine biogeochemical modeling. Global Biogeochemical Cycles 13 (3), 705–714.

Dugdale, R.C., Wilkerson, F.P., Minas, H.J., 1995. The role of a silicate pump in driving new production. Deep-Sea Research Part I—Oceanographic Research Papers 42 (5), 697–719.

Erickson, D.J., Hernandez, J.L., Ginoux, P., Gregg, W.W., McClain, C.R., Christian, J., 2003. Atmospheric iron delivery and surface ocean biological activity in the Southern Ocean and Patagonian region. Geophysical Research Letters 30 (12), 1609.

Gaiero, D.M., Probst, J.L., Depetris, P.J., Bidart, S.M., Leleyter, L., 2003. Iron and other transition metals in Patagonian riverborne and windborne materials: geochemical control and transport to the southern South Atlantic Ocean. Geochimica et Cosmochimica Acta 67 (19), 3603–3623.

Garcia, C.A.E., Sarma, Y.V.B., Mata, M.M., Garcia, V.M.T., 2004. Chlorophyll variability and eddies in the Brazil-Malvinas Confluence region. Deep-Sea Research Part II—Topical Studies in Oceanography 51 (1–3), 159–172.

Gasso, S., Stein, A.F., 2007. Does dust from Patagonia reach the sub-Antarctic Atlantic ocean? Geophysical Research Letters 34, L01801.

Grasshoff, K., Ehrhardt, M., Kremling, K., 1983. Methods of Seawater Analysis. Verlag Chemie, Weinheim, 419pp.

Gregg, W.W., Casey, N.W., McClain, C.R., 2005. Recent trends in global ocean chlorophyll. Geophysical Research Letters 32, L03606.

Hegarty, S.G., Villareal, T.A., 1998. Effects of light level and N:P supply ratio on the competition between Phaeocystis cf. *pouchetii* (Hariot) Lagerheim (Prymnesiophyceae) and five diatom species. Journal of Experimental Marine Biology and Ecology 226 (2), 241–258.

Holligan, P.M., et al., 1993. A biogeochemical study of the Coccolitho-phore, Emiliania huxleyi, in the North-Atlantic. Global Biogeochem-ical Cycles 7 (4), 879–900.

Klausmeier, C.A., Litchman, E., Daufresne, T., Levin, S.A., 2004. Optimal nitrogen-to-phosphorus stoichiometry of phytoplankton. Nature 429, 171–174.

Koroleff, F., 1969. Direct determination of ammonia in natural waters as indophenol blue. ICES C.M. 1969/C: 9. Hydrology Communication, p. 4.

Loder, J., Petrie, B., Gawarkiewicz, G., 1998. The coastal ocean off northeastern North America: a large-scale view. In: Robinson, A.R., Brink, K.H. (Eds.), The Sea, vol. 11. pp. 105–133.

Longhurst, A., 1998. The Ecological Geography of the Sea. Academic Press, Elsevier, Amsterdam, New York, 424pp.

Loscher, B.M., de Baar, H.J.W., de Jong, J.T.M., Veth, C., Dehairs, F., 1997. The distribution of Fe in the Antarctic circumpolar current. Deep-Sea Research II 44, 143–187.

Martos, P., Piccolo, M.C., 1988. Hydrography of the Argentine Continen-tal-Shelf between 38-degrees-S and 42-degrees-S. Continental Shelf Research 8 (9), 1043–1056.

Matano, R.P., Palma, E.D., 2008. The upwelling of downwelling currents. Journal of Physical Oceanography, in press.

Moisan, T.A., Mitchell, B.G., 1999. Photophysiological acclimation of Phaeocystis antarctica Karsten under light limitation. Limnology and Oceanography 44 (2), 247–258.

Moore, J.K., Doney, S.C., Kleypas, J.A., Glover, D.M., Fung, I.Y., 2002. An intermediate complexity marine ecosystem model for the global domain. Deep-Sea Research Part II—Topical Studies in Oceanography 49, 403–462.

Margalef, R., 1962. Succession in marine populations. Adv. Front. Pl. Sci. 2137–2188.

Negri, R.M., Carreto, J.I., Benavides, H.R., Akselman, R., Lutz, V.A., 1992. An unusual bloom of *Gyrodinium* cf. *aureolum* in the Argentine Sea—community structure and conditioning factors. Journal of Plankton Research 14 (2), 261–269.

Palma, E.D., Matano, R.P., Piola, A.R., 2004. A numerical study of the Southwestern Atlantic Shelf circulation: barotropic response to tidal and wind forcing. Journal of Geophysical Research—Oceans 19, C08014.

Parsons, T.R., Maita, Y., Lalli, C.M., 1984. A Manual of Chemical and Biological Methods for Seawater Analysis. Pergamon Press, Oxford, 173pp.

Peterson, R.G., Whitworth III, T., 1989. The Subantarctic and Polar Fronts in relation to the deep water masses through the Southwestern Atlantic. Journal of Geophysical Research 94 (C8), 10817–10838.

Piola, A.R., Gordon, A.L., 1989. Intermediate waters in the southwest South Atlantic. Deep-Sea Research 36, 1–16.

Platt, T., Gallegos, C.L., Harrison, W.G., 1980. Photoinhibition of photosynthesis in natural assemblages of marine-phytoplankton. Journal of Marine Research 38 (4), 687–701.

Platt, T., Sathyendranath, S., White, G.N., Ravindran, P., 1994. Attenuation of visible-light by phytoplankton in a vertically structured ocean—solutions and applications. Journal of Plankton Research 16 (11), 1461–1487.

Podestá, G.P., 1990. Migratory pattern of Argentine Hake Merluccius hubbsi and oceanic processes in the Southwestern Atlantic Ocean. Fisheries Bulletin 88 (1), 167–177.

Pondaven, P., Ruiz-Pino, D., Druon, J.N., Fravalo, C., Treguer, P., 1999. Factors controlling silicon and nitrogen biogeochemical cycles in high nutrient, low chlorophyll systems (the Southern Ocean and the North Pacific): comparison with a mesotrophic system (the North Atlantic). Deep-Sea Research Part I—Oceanographic Research Papers 46 (11), 1923–1968.

Redfield, A.C., Ketchum, B.H., Richard, F.A., 1963. The influence of organisms on the composition of sea-water. In: Hill, M.N. (Ed.), The Sea. Wiley-Interscience, New York, pp. 26–77.

Rivas, A.L., 2006. Quantitative estimation of the influence of surface thermal fronts over chlorophyll concentration at the Patagonian shelf. Journal of Marine Systems 63, 183–190.

Rivas, A.L., Dogliotti, A.I., Gagliardini, D.A., 2006. Seasonal variability in satellite-measured surface chlorophyll in the Patagonian Shelf. Continental Shelf Research 26, 703–720.

Rodhouse, P.G., Elvidge, C.D., Trathan, P.N., 2001. Remote sensing of the global light-fishing fleet: an analysis of interactions with oceanography, other fisheries and predators. Advances in Marine Biology 39, 261–303.

Romero, S.I., Piola, A., Charo, M., Garcia, C.A.E., 2006. Chlorophyll a variability off Patagonia based on SeaWiFS data. Journal of Geophysical Research—Oceans 111, C05021.

Rost, B., Riebesell, U., 2004. Coccolithophores and the biological pump: responses to environmental changes. In: Thierstein, H.R., Young, J.R. (Eds.), Coccolithophores: From Molecular Processes to Global Impact. Springer, Berlin, pp. 99–125.

Saraceno, M., Provost, C., Piola, A.R., Bava, J., Gagliardini, A., 2004. Brazil Malvinas Frontal System as seen from 9 years of advanced very high resolution radiometer data. Journal of Geophysical Research—Oceans 109 (C5).

Saraceno, M., Provost, C., Piola, A.R., 2005. On the relationship between satellite-retrieved surface temperature fronts and chlorophyll a in the western South Atlantic. Journal of Geophysical Research—Oceans 110, C11016.

Sarthou, G., Timmermans, K.R., Blain, S., Treguer, P., 2005. Growth physiology and fate of diatoms in the ocean: a review. Journal of Sea Research 53, 25–42.

Schloss, I.R., et al., 2007. Role of plankton communities in sea–air variations in $pCO(2)$ in the SW Atlantic Ocean. Marine Ecology—Progress Series 332, 93–106.

Signorini, S., Garcia, V.M.T., Piola, A.R., Garcia, C.A.E., Mata, M.M., McClain, C.R., 2006. Seasonal and interannual variability of calcite in the vicinity of the Patagonian Shelf Break ($38°S–52°S$). Geophysical Research Letters 33, L1,6610.

Steemann, N.E., 1952. The use of radioactive carbon (^{14}C) for measuring organic production in the sea. Journal du Conseil Permanent International pour l' Exploration de la Mer 18, 117–140.

Strickland, J.D.H., Parsons, T.R., 1972. A practical handbook of seawater analysis. Bulletin of the Fisheries Research Board of Canada 167, 331pp.

Sverdrup, H.U., 1953. On conditions for the vernal blooming of phytoplankton. Journal du Conseil Permanent International d' Exploration de la Mer 18, 287–295.

Takahashi, T., et al., 2002. Global sea–air CO_2 flux based on climatological surface ocean $pCO(2)$, and seasonal biological and temperature effects. Deep-Sea Research Part II—Topical Studies in Oceanography 49, 1601–1622.

Utermöhl, H., 1958. Zur Vervollkomnung der quantitativen Phytoplankton-Metodik. Mitteilungen-Internationale Vereiningong Für Limnologie 9, 1–38.

Welschmeyer, N.A., 1994. Fluorometric analysis of chlorophyll-a in the presence of chlorophyll-b and pheopigments. Limnology and Oceanography 39 (8), 1985–1992.

Windom, H.L., Moore, W.S., Niencheski, L.F.H., Jahrike, R.A., 2006. Submarine groundwater discharge: a large, previously unrecognized source of dissolved iron to the South Atlantic Ocean. Marine Chemistry 102 (3/4), 252–266.